Anais XIII Simpósio Brasileiro de Sensoriamento Remoto, Florianópolis, Brasil, 21-26 abril 2007, INPE, p. 4727-4734.

Complex EOF and wavelet analysis of sea surface temperature anomaly images in the Southwestern Atlantic Ocean from 1985 to 2004

Ronald Buss de Souza [1]
David Cromwell [2]
Carlos Alessandre Domingos Lentini [3]

[1] Instituto Nacional de Pesquisas Espaciais - INPE
Av. dos Astronautas 1758, 12227-010, São José dos Campos, Brazil
ronald@dsr.inpe.br

[2] Ocean Observing and Climate
National Oceanography Centre, Southampton (NOCS)
European Way, Southampton, SO14 3ZH, United Kingdom
ddc@noc.soton.ac.uk

[3] Fundação Cearense de Meteorologia e Recursos Hídricos (FUNCEME)
Av. Rui Barbosa 1246, 60115-221, Fortaleza, Brazil
lentini@funceme.br

Abstract. Satellite-derived SST data from January l985 to December 2004 were obtained from the NOAA Pathfinder Project at a spatial resolution of 4 km. Monthly data together with 20-year long climatological means were used to produce sea surface temperature anomaly (ASST) images for the Southwestern Atlantic Ocean. The variability of the ASST fields was analyzed using Complex Empirical Orthogonal Function (CEOF) and wavelet methods to account for the main modes of variability. The most energetic peaks found in the series were centered at ~1 year, ~3.5 years, ~6 years and ~7 years. While the first is a known dominant peak for the SST fields of the region, the last ones are not very well documented and may be related to large scale forcing. Some ASST peaks are coincident in time with the El Niño events of 1987 and 1998. The first five CEOF modes, however, summed up to only ~35% of the total variance of the ASST fields of the region: a sign that our study area is very inhomogeneous as previously reported in the literature.

Keywords: Complex EOF, sea surface temperature, Southwestern Atlantic Ocean, ocean variability.

1. Introduction

The Southwestern Atlantic Ocean (SWA) is considered one of the most active regions of the World Ocean (Chelton et al., 1990). This region comprises different ocean regimes mainly related to the Brazil-Malvinas Confluence (BMC) and to coastal waters mainly originated from the La Plata river. At the BMC the poleward warm, saline Brazil Current (BC) meets the Equatorward cold, fresher Malvinas Current (MC). The dynamics of the BMC region can be characterized by the very strong gradients of sea surface temperature (SST) between BC and MC waters. The behavior of the SST fields in the BMC region has been widely described in the literature especially with the help of satellite data (recent papers include Lentini et al., 2002; Souza and Robinson, 2004; Souza et al., 2006).

Provost and Le Traon (1993) report the high inhomogenity and anisotropy of the BMC region at the mesoscale. At shorter frequencies, the BMC variability is very strong being mainly dominated by the annual and the semi-annual periods (Fu, 1996). Podestá et al. (1991) report that the annual cycle is responsible for the majority of the SST variability in the Southwestern Atlantic. The authors also report that more than 80 % of all the SST variability on the continental shelf off the Southwestern Atlantic Ocean is accounted by the seasonal (annual) cycle.

Goni et al. (1996) described the BMC SST annual cycle with amplitudes ranging from 8 ^{o}C in winter to about 25 ^{o}C in summer at the core of BC. Podestá et al. (1991) report that the annual cycle dominates the variability of the SST fields present at the Southwestern Atlantic Ocean. Higher amplitudes of the SST signal (10^{o}C to 13^{o}C) were found at the La Plata estuary and at continental shelf south of it. Lentini et al. (2000) estimated SST annual amplitudes ranging from 4^{o}C to 13^{o}C along the shelf from the La Plata estuary and northwards up to 23^{o}S. The authors report that most of this variation is due to a higher BC transport during summer and a higher MC transport during winter.

Despite the good characterization of the SST variability at the BMC region and continental shelf off Southern South America, little is known about the dynamics of the oceanographic processes occurring at the coastal region. The fate of the La Plata outflow waters at the continental shelf off the estuary is still a matter of constant research (e.g. Guerrero et al., 1997; Zavialov and Möller, 2000, Gonzalez-Silvera et al., 2006). Souza and Robinson (2004) acknowledge that the waters dominating the continental shelf in southern Brazil are marked by their strong interannual variability. According to these authors, the seasonal changes of the vertical and horizontal water mass structure of the coastal waters may be not only directly related to the local winds and the La Plata discharge, but also to the variability of the BMC off the continental shelf.

The objective of the present paper is to describe the temporal and spatial variability of the SST fields at the Southwestern Atlantic Ocean including the costal regions off Southern South America and the BMC region. We use novel, global satellite-derived SST data available at umprecedently high spatial resolution. The data series is also long enough for climatological analysis of the area being available for a 20 years long period between 1985 and 2004. This data is free of cloud coverage and especially prone for coastal studies which can shed new light at the spatial discrepancies between the variability patterns of the BC, MC and coastal domains in the Southwestern Atlantic Ocean. We use Complex Empirical Orthogonal Function (CEOF) analysis to account for the major modes of spatial and temporal variability present in the SST fields. Temporal analysis of the major modes of oscillation in the study area is made using wavelet analysis. The data and methodology used here are presented in Section 2. Section 3 presents the results; discussion is made in section 4 while section 5 summarizes our major conclusions.

2. Data and Methods of analysis

2.1. Satellite data and study area

The SST data used here is the Pathfinder v.5 (PV5 hereafter) product. This data set is derived from raw data collected by the AVHRR radiometers onboard the NOAA satellites from the NOAA-9 to the present. The data sets represent a historical reprocessing of the entire AVHRR time series using consistent SST algorithms, improved satellite and inter-satellite calibration, quality control and cloud detection (NODC/SOG, 2006). PV5 provides nightly and daily global SSTs at a spatial resolution near to 4 km x 4 km (Vazquez et al., 1998; Kilpatrick et al., 2001). The data is provided on equal-angle, longitude-latitude grids of 8192 by 4096 pixels. For this work we used 240 global, monthly mean SST images available for the period between January 1985 to December 2004. We also used 12 climatological SST images representing the climatological months January to December. PV5 images were downloaded from <http://pathfinder.nodc.noaa.gov>.

Global images were cut into a consistent area in the SWA comprising 20^{o}S to 45^{o}S, 60^{o}W to 45^{o}W (**Figure 1a**). Anomalies of SST (ASST) were computed for each of the 240 monthly SST images of the study region subtracting the last from the climatological images of each month. Unfortunately, our study area presents a known problem with the land mask

(NODC/SOG, 2006): two areas are incorrectly classified as land (islands) off the east coast of South America, around the Patagonian continental shelf (around 40°S - 44°S and 60°W - 55°W). This causes the loss of SST (and, consequently ASST) data at the false islands location.

2.2. CEOF and wavelet analysis

One of the best applications of the Empirical Orthogonal Function (EOF) analysis is to help identifying the major common characteristics in a large data set such as our 240 ASST images. This data set is statistically decomposed into its major modes of variability which are obtained from an eigenvalue analysis of the data covariance matrix. As a result from the EOF analysis, eigenvectors and their associated Principal Components (PCs) are generated. Eigenvectors are mapped to describe the spatial variability of the studied data while the PCs are used to describe the temporal variability of the associated spatial field (Cromwell, 2006).

Complex EOF (CEOF) analysis is recommended when we need information not only about the amplitudes but also about the phase of the studied parameter (Fu, 2004). Cromwell (2006) describes how the method "complexify" the original "real" data generating statistical patterns containing both real and imaginary components. These components physically represent the amplitudes and phase, respectively. Progression in time corresponds to anti-clockwise rotation of the eigenvector phase. Owing to computational limitations, ASST data were regridded from the original 4 km x 4 km resolution to 0.2 x 0.2 degrees using a Gaussian interpolation scheme. Although degraded from the original PV5 resolution, the amplitude fields from the COEF analysis used here proved enough for discriminating most of the known activities in the BCM and coastal regions. The main parameters for the Gaussian interpolation were (a) full-width half-maximum = 20 km and (b) search radius = 30 km.

As a result of the CEOF analysis, we generated maps of the complex-valued spatial variability patterns (amplitudes and phase) of the SWA ASSTs. The associated complex PCs were plotted as time series of amplitude and phase. The spectral content of the amplitude and phase time series were analyzed using an adaptation of the Morlet wavelet method as described by Cromwell (2006). Briefly, the wavelet analysis allows one to locate power variations within a discrete time series in a range of scales. The wavelet analysis provides two kinds of power spectra: (a) the local wavelet power spectrum given by the square of the wavelet coefficients and (b) the global wavelet spectrum which is the averaged spectrum over all time.

3. Results

Figure 1 shows the study area and the spatial patterns of the first five CEOFs of the 1985-2004 ASST fields. Amplitudes (arbitrary units) are plotted as colored contours while phases are denoted by the associated arrows. The first CEOF (CEOF1) represents 14.3% while modes two to five account for 9.3%, 5%, 3.2% and 3% of the total variability of the SST fields, respectively (**Table 1**). The first 5 modes sum up to only ~35% of the total variance: a sign that our study area is very inhomogeneous as reported by Provost and Le Traon (1993).

The spatial patterns of CEOF1 amplitude show high variability at the coastal regions (**Figure 1a**). Low amplitudes are found at the BC domain including the coastal regions at latitudes lower than Santa Marta Cape (~28°S) and the BC retroflection at the BMC region. The MC core and a path centered at ~42°S, 45°W present intermediate amplitudes. All domain of the study area is in phase. The second CEOF (CEOF2) presents a spatial pattern with high amplitudes at both the southern and the northern part of the study area at the MC and BC domains, respectively. The low amplitudes are located at the BMC region. The BC

and MC domains are in opposite phase. The third CEOF (CEOF3) shows strong variability at most of the coastal regions. A path of very high amplitudes is also found centered at ~40°S, 45°W. Low variability is found at the BC domain and at the MC core. The coastal regions are in opposite phase with the patch near 45°W. The fourth and fifth CEOF modes (CEOF4, CEOF5) show many eddy-like patches of variability.

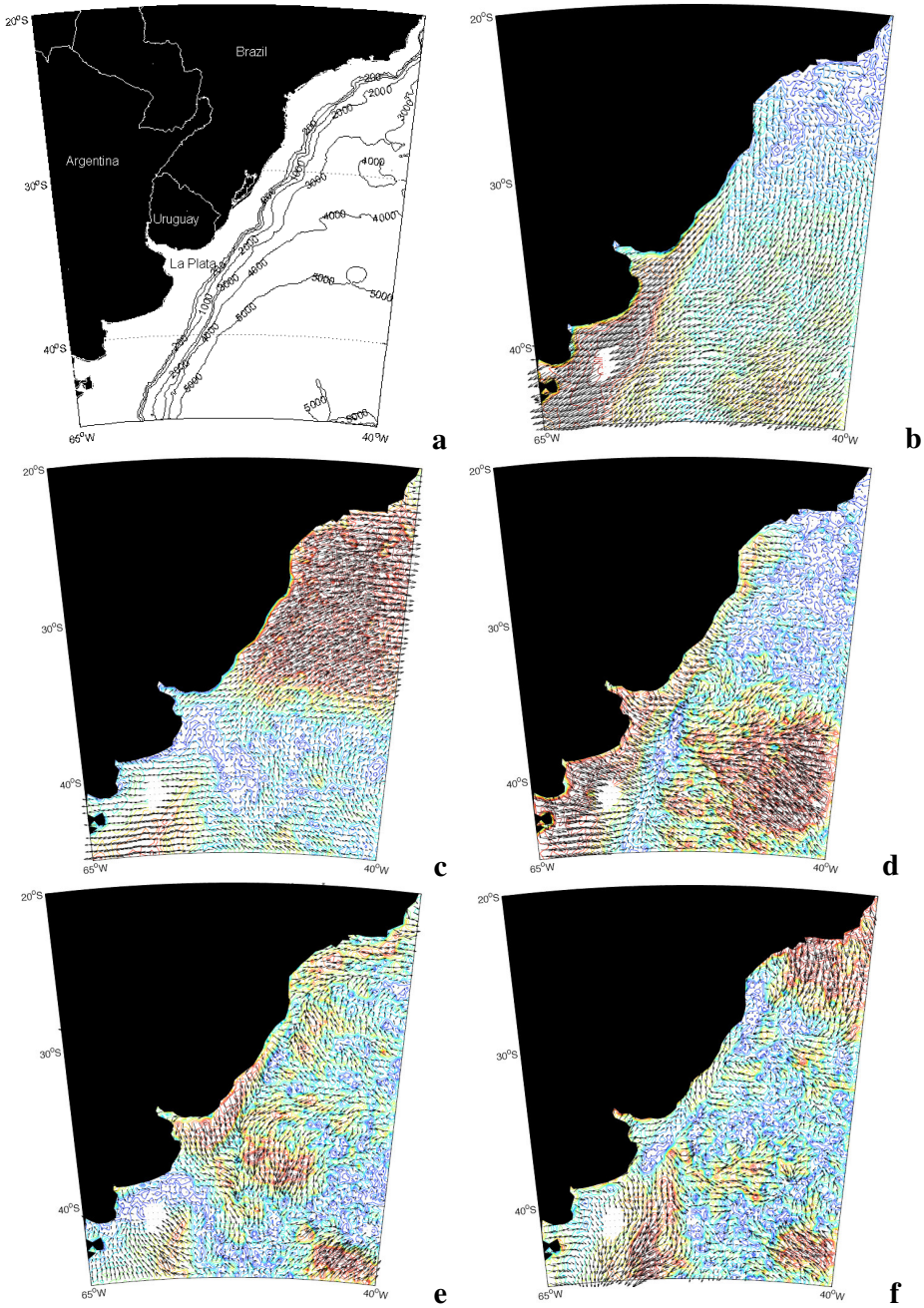

Figure 1. (a) Study area at the SWA with bathymetry (meters); (b-f) CEOF1 to CEOF5, respectively.

Table 1 summarizes the characteristics of the first 3 CEOF modes (representing most of the variance of the series) presented in **Figure 1**. The dominant periods related to the

amplitude and phase time series were computed by the wavelet analysis. **Figure 2** shows the wavelet results for CEOF1 PC time series. Results for the other modes are not show due to space restrictions. Most of the global wavelet spectra for all modes show a period centered at the vicinity of the annual cycle. Although working with the SST anomalies, the presence of this annual cycle in the series may be related to the interannual variability of the cycle, which causes it to depart from the exact yearly period every calendar year.

Table 1. Characteristics of the leading three CEOF modes of monthly ASSTs of the SWA for the period between January 1985 and December 2004.

Mode and percentage of variability	Dominant timescales
1: 14.3 %	~1, ~3.5, ~7 yr (amplitude); ~2 yr, ~0.25-0.5 yr (phase) **Temporal pattern** 1-yr cycle strong between 1988-1995 Marked 2-yr cycle from 1998-2002 ~0.25-0.5 yr strong between ~1992-1994
2: 9.3 %	~1 yr, ~1.5-6 yr (amplitude); ~1-2 yr (phase) **Temporal pattern** ~1 yr marked between 1986-1988 ~1.5-6 yr strong in latter half of time series (~1995 onwards) ~1-2 yr strong between 1988-1992 and again 2000-2003
3: 5.0 %	~0.5-1.5 yr, ~6 yr (amplitude); ~0.5 yr, ~1 yr (phase) **Temporal pattern** ~0.5-1.5 yr marked during 1990-1994; 1997-1999; 2001-2004 ~6 yr above cone of influence in middle of time series ~0.5 yr marked 1986-1987; 1991; 1998-2000 ~1 yr 1993-1995; 1998-1999

4. Discussion

The presence of the annual cycle found here for the SWA (**Table 1**) has been demonstrated by several authors (e.g. Olson et al., 1988; Podestá et al., 1991; Podestá, 1997). As for the spatial variability, Goni et al. (1996), Provost et al. (1992) and Provost and Le Traon (1993), for example, also indicated the presence of a region of high SSH and SST variability centered at about 40°S, 55°W in agreement to our data (**Figure 1d**). The interannual and intrannual cycles of the SWA are also described by several authors (e.g. Provost et al., 1992; Campos et al., 1999; Vivier and Provost, 1999a, 1999b, among others). Among the peaks of variability found on the region, some may be related to ENSO events.

Campos et al. (1999) compared ASSTs computed for the period between 1982 and 1994 at a particular location of the SWA (26°15'S, 47°43'W) with monthly means of the Southern Oscillation Index (SOI) for the same period. The authors found two peaks of high coherence between the ASSTs and SOI series at the ~0.7 years and 1.5 years periods. These periods are generally found here (**Table 1**).

Lentini et al. (2001) also investigated the relation between ENSO events and the SWA SST variability. The authors report that there is a tendency of cold SSTA to be related to ENSO events. Measurements of ASST variability were also performed by Lentini et al. (2001) by means of EOF analysis. They used SSTA data from along-shelf transects in the SWA. The first EOF mode of transects taken at the SWA continental shelf present a spatial variability very consistent to the results presented here (**Figure 1b**) where all coastal domain

is in phase and the higher amplitudes are found to the south of Santa Marta Cape. The second EOF mode of the continental shelf transects of Lentini et al. (2001), on the other hand, presents a nodal point (zero amplitude) centered at 32°S. Positive amplitudes are found north of this location while negative amplitudes are located to the south. This opposition of phases is similar to the one presented at the coastal regions of our CEOF2 (**Figure 1c**) although our nodal point is located a little farther south at ~35°S.

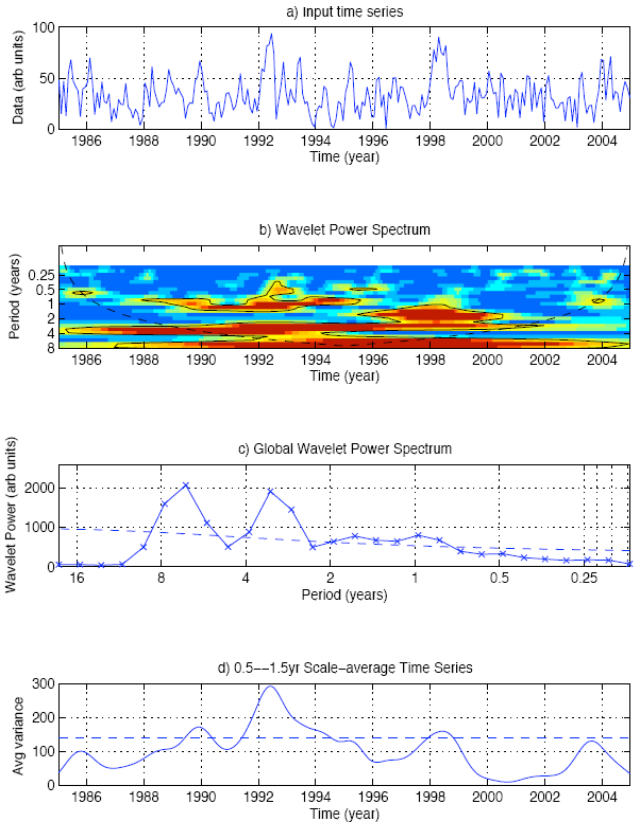

Figure 2. Wavelet analysis of PC amplitude associated with CEOF1. **(a)** amplitude time series of CEOF1; **(b)** wavelet power spectrum of (a); **(c)** global wavelet spectrum; **(d)** time series of scale average of (b) for periods in range 0.5-1.5 years. In (b), the dashed line indicates the cone of influence, below which edge effects become important, and the solid contour is the 95% confidence level. In (c) and (d), the 95% confidence level is indicated by a dashed line.

5. Conclusion

The variability of the satellite-derived ASST fields of the Southwestern Atlantic Ocean has been analyzed here. We used the CEOF and wavelet methods to account for the main modes of variability. We described the spatial variability of the representative ASST domains describing amplitudes and differences in their phases.

Most energy peaks found here have been previously described for the region, although periods at lower frequencies (higher periods) are still to be better studied. From these, we highlight the periods centered at ~3.5 years, ~6 years and ~7 years which may be related to large scale forcing. Future work includes the investigation of these peaks with respect to other atmospheric and oceanographic variables such as the wind, atmospheric pressure and currents,

for example. We are also prone to investigate the CP time series with respect to known El Niño indexes such as the SOI, the Niño 3.4 (Trenberth, 1997) and the Multivariate El Niño Index (MEI – Wolter and Timlin, 1998).

This work also demonstrated the utility of the PV5 product to study the ASST fields of the SWA. The work shows differences between the coastal and oceanic regimes in this part of the World Ocean. Better results on the interannual variability of the series may be obtained by filtering the original PC series for periods shorter than 1.5 years. The present results can be applied in the future to better understand the relation between environmental parameters and the local fisheries, for example.

Acknowledgements. The authors are thankful to CNPq for supporting this research through the Brazilian Antarctic Program, INTERCONF project (No. 557284/05-8). Data were provided by NOAA Pathfinder Project. Computer routines used here were available from the Ocean Observing and Climate Group, National Oceanography Centre, Southampton, UK. We also thank Com. Parente from R/V Ary Rongel for supporting our research.

References

Campos, E.J.D., Lentini, C.D.; Miller, J.L.; Piola, A.R. Interannual variability of the sea surface temperature in the South Brazil Bight. **Geophysical Research Letters**, v. 26, n. 14, p. 2061-2064, 1999.

Chelton, D.B.; Schlax, M.G.; Witter, D.L.; Richman, J.G. GEOSAT altimeter observations of the surface circulation of the Southern Ocean, **Journal of Geophysical Research**, v. 95, p. 17877-17903, 1990.

Cromwell, D. Temporal and spatial characteristics of sea surface height variability in the North Atlantic Ocean. **Ocean Science Discussions**, v. 3, p. 609-636, 2006.

Fu, L.-L. The circulation and its variability of the South Atlantic Ocean: first results from the TOPEX/POSEIDON mission. In: Wefer, G.; Berger, W.H.; Siedler, G.; Webb, D.J. (Eds.), **The South Atlantic: Present and past circulation**, (p. 63-82). Springer-Verlag, Berlin, 644 p., 1996.

Fu, L-L. The interannual variability of the North Atlantic Ocean revealed by combined data from TOPEX/Poseidon and Jason altimetric measurements. **Geophysical Research Letters**, 31:L23303, doi:10.1029/2004GL021200, 2004.

Goni, G.; Kamholz, S.; Garzoli, S.; Olson, D. Dynamics of the Brazil-Malvinas Confluence based on inverted echo sounders and altimetry. **Journal of Geophysical Research**, v. 101(C7), p.16273-16289, 1996.

Gonzalez-Silvera, A.; Santamaria-del-Angel, E.; Millán-Núñez, R. Spatial and temporal variability of the Brazil-Malvinas Confluence and the La Plata Plume as seen by SeaWiFS and AVHRR imagery. **Journal of Geophysical Research**, v. 111, C06010, doi:10.1029/2004JC002745, 2006.

Guerrero, R.A.; Acha, E.M.; Framiñan, M.B.; Lasta, C.A. Physical oceanography of the Rio de la Plata Estuary, Argentina. **Continental Shelf Research**, v. 17, n. 7, p.727-742, 1997.

Kilpatrick, K.A., Podestá, G.P. Evans, R. Overview of the NOAA/NASA Advanced Very High Resolution Radiometer Pathfinder algorithm for sea surface temperature and associated matchup database, **Journal of Geophysical Research**, v. 106(C5), p. 9179-9197, 2001.

Lentini, C.A.D.; Podestá, G.; Olson, D.B.; Campos, E.J.D. Sea surface temperature anomalies on the Western South Atlantic from 1982 to 1994, **Continental Shelf Research**, v. 21, p. 89-112, 1991.

Lentini, C.A.D.; Olson, D.B.; Podestá, G. Statistics of Brazil Current rings observed from AVHRR: 1993 to 1998, **Geophysical Research Letters**, v. 29, n. 16, p. 58-1 – 58-4, 2002.

Lentini, C.A.D.; Campos, E.J.D.; Podestá, G. The annual cycle of satellite derived sea surface temperature on the western South Atlantic shelf, **Brazilian Journal of Oceanography**, v. 48, n. 2, p. 93-105, 2000.

Olson, D.B.; Podestá, G.P.; Evans, R.H.; Brown, O. B. Temporal variations in the separation of Brazil and Malvinas currents. **Deep-Sea Research**, v. 35, n. 12, p.1971-1990, 1988.

NODC/SOG. **4 km Pathfinder Version 5.0 User Guide**. NOAA Satellite and Information Service, National Oceanographic Data Center, NODC Satellite Oceanography Group, 2006. Available at: <http://www.nodc.noaa.gov/sog/pathfinder4km/userguide.html>. Last consulted: 26 Jun 2006.

Podestá, G. Utilización de datos satelitarios en investigaciones oceanográficas y pesqueras en el Océano Atlántico Sudoccidental. In: Boschi, E.E. (Ed.), **El mar argentino y sus recursos pesqueros, Tomo 1, Antecendentes históricos de las exploraciones en el mar y las características ambientales**. INIDEP, Secretaría de Agricultura, Ganadería, Pesca y Alimentación, Mar del Plata, Argentina, 1997.

Podestá, G.P.; Brown, O.B.; Evans, R.H. The annual cycle of satellite-derived sea surface temperature in the southwestern Atlantic Ocean. **Journal of Climate**, v. 4, p. 457-467, 1991.

Provost, C.; Garcia, O.; Garçon, V. Analysis of satellite sea surface temperature time series in the Brazil-Malvinas Current Confluence region: Dominance of the annual and semiannual periods. **Journal of Geophysical Research**, v. 97(C11), p. 17841-17858, 1992.

Provost, C.; Le Traon, P-Y. Spatial and temporal scales in altimetric variability in the Brazil-Malvinas Current Confluence region: Dominance of the semiannual period and large spatial scales. **Journal of Geophysical Research**, v. 98(C10), p. 18037-18051, 1993.

Souza, R.B.; Robinson, I.S. Satellite and Lagrangian observations of the Brazilian Coastal Current, **Continental Shelf Research**, v. 24, p.241-262, 2004.

Souza, R.B.; Mata, M.M.; Garcia, C.A.E.; Kampel, M.; Oliveira, E.N.; Lorenzzetti, J.A. Multi-sensor satellite and *in situ* measurements of a warm core eddy south of the Brazil-Malvinas Confluence region. **Remote Sensing of Environment**, v. 100, p. 52-66, doi:10.1016/j.rse.2005.09.018, 2006.

Trenberth, K. E. The Definition of El Niño. **Bulletin of the American Meteorology Society**, v. 78, p. 2771-2777, 1997.

Vivier, F.; Provost, C. Volume transport of the Malvinas Current. Can the flow be monitored by TOPEX/POSEIDON? **Journal of Geophysical Research**, v. 104(C9), p. 21105-21122, 1999a.

Vivier, F.; Provost, C. Direct measurements in the Malvinas Current. **Journal of Geophysical Research**, v. 104(C9), p. 21083-21103, 1999b.

Vazquez, J.; Perry, K.; Kilpatrick, K. A. **NOAA/NASA AVHRR Oceans Pathfinder, Sea Surface Temperature Data Set, User's Reference Manual, Version 4.0**. Pasadena: Jet propulsion Laboratory, 1998. (JPL Publication D-14070).

Wolter, K., Timlin, M.S. Measuring the strength of ENSO - how does 1997/98 rank? **Weather**, v. 53, p. 315-324, 1998.

Zavialov, P.O.; Möller, O.O. Modeling and observations of currents off Southern Brazil and Uruguay: the Rio Grande Current. In: Zatsepin, A.G. (Ed.), **Oceanic Fronts and Related Phenomena** (Proc. of Fedorov International Memorial Symposium). IOC Workshop Report No. 159, UNESCO, GEOS, Moscow, p. 612-617, 2000.